Al-Mukhtar Journal of Basic Sciences 24 (2): 149-157, 2026
Doi: https://doi.org/10.54172/f992sy26

Research Article

Open Access

Estimation of Annual Gonadal Equivalent Dose (AGDE) and Radiological Hazards of Granite Samples

Asma M.A. Othman[1*] Areej I. Hazawi[2] and Salha D.Y. Alsaadi [3]

*Corresponding author: asma.alabrdi@omu.edu.ly Department of Physics, Faculty of Sciences Omar Al-Mukhtar university, Libya

[2, 3] Department of Physics, Faculty of Sciences Omar Al-Mukhtar university, Libya

Received:
11 June 2026

Accepted:
22 August 2026

Publish online:
31 August 2026

Abstract
This study investigates the specific activity concentrations of ^{226}Ra, ^{232}Th, and ^{40}K radionuclides in six granite samples collected from the Eastern Desert of Egypt. Measurements were performed using a High-Purity Germanium (HPGe) gamma-ray spectrometer. To evaluate environmental external radiation hazards and ensure radiological safety, key standard indices were calculated, including the Annual Gonadal Dose Equivalent (AGDE), Gamma Representative Level Index (RLI), Activity Utilization Index (AUI), Concentration Index (Ic), Alpha Index (Iα), and the External and Internal Annual Effective Dose Equivalents (AEDE). The evaluation of ingestion doses was omitted because granite serves strictly as an architectural, decorative, and structural building material and does not enter the biological food chain. The experimental results revealed that the radioactivity concentrations and all related radiological risk assessment indices significantly exceed the internationally recommended public exposure safety limits established by UNSCEAR. Specifically, the average AGDE was determined to be 8156.95 $\mu Sv \cdot y^{-1}$, which is approximately 27 times greater than the global average background limit (300 $\mu Sv \cdot y^{-1}$). These findings strongly indicate that the studied granite varieties present a substantial external radiological hazard and must be managed with strict environmental regulatory oversight in premium commercial, industrial, and residential architectural applications.

Keywords: Natural radioactivity; Granite materials; Annual Gonadal Dose Equivalent (AGDE); HPGe gamma spectroscopy; Radiological hazard indices; Public health risk.

INTRODUCTION

Natural background radiation originates predominantly from primordial terrestrial radionuclides distributed within the Earth's crust, namely uranium-238 (^{238}U) and thorium-232 (^{232}Th) decay series, along with primordial potassium-40 (^{40}K). Granite rocks, which are widely distributed across the Egyptian Nubian Shield, are widely utilized worldwide as high-end building materials, pavements, structural facades, and internal ornamental decorations (Moghazy et al., 2021). Due to their igneous plutonic origin, granites inherently contain elevated activity levels of these natural radioisotopes compared to other sedimentary rocks (Abd El-halim et al., 2017). Consequently, evaluating the ambient occupational and public external gamma-ray radiation hazards associated with the commercial exploitation of these materials is essential to maintain standard indoor and outdoor exposure thresholds below safety criteria (Shereif et al., 2026).

The Author (s) 2026. This article is distributed under the terms of the Creative Commons Attribution-NonCommercial 4.0 International License [http://creativecommons.org/licenses/by-nc/4.0/], which permits unrestricted use, distribution, and reproduction in any medium, for non-commercial purposes only*, provided you give appropriate credit to the original author(s) and the source, provide a link to the Creative Commons license, and indicate if changes were made.

In accordance with modern environmental radiation protection standards, the evaluation of human radiological risks must match the realistic exposure pathways of the target matrix. The primary aim of this work is to provide a highly precise assessment of specific activity concentrations in representative Egyptian granite varieties, compute standard structural hazard indices such as the Annual Gonadal Dose Equivalent (AGDE), Representative Level Index (RLI), and Activity Utilization Index (AUI), and provide a solid geological justification for the observed radiological trends.

MATERIALS AND METHODS

Sampling and geological description:

A total of 6 granite samples were strategically collected from the Eastern Desert of Egypt. Geologically, the study area contains the main types of granite formations.

1. Altered granite: Mainly present in the west and composed primarily of biotite and muscovite granodiorite.
2. Young granite: coarse- to medium-grained pink granite. Color ranges from bright pink to reddish-pink in fresh specimens, changing to pale or reddish-brown hues along shear zones and fracture intervals as a result of hydrothermal alteration processes. - Laboratory preparation

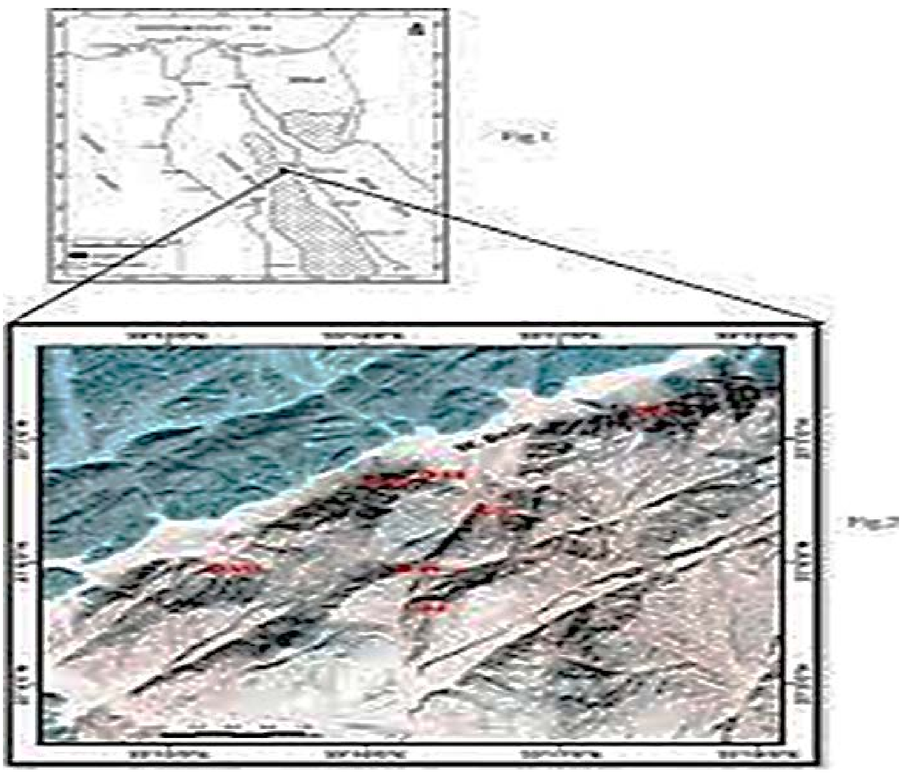

Figure (1). Location map of the Eastern Desert of Egypt

Six distinct commercial granite varieties were collected from the Eastern Desert of Egypt. Each sample was crushed, homogenized, sieved through a 1-mm mesh, and dried in a temperature-controlled oven at 110 °C for 24 hours to eliminate moisture content. The prepared samples were then sealed hermetically in standard cylindrical Maronelli beakers and stored for at least four weeks to achieve secular radioactive equilibrium between radium-226 (^{226}Ra), thorium-232 (^{232}Th), and their respective short-lived daughter products.

Table (1). Description of granite samples

Samples No	Description
G1	Alkali granite
G2	Biotite granite
G3	Hornblende granite
G4	Porphyritic granite
G5	Graphic granite
G6	Muscovite granite

Gamma-Ray Spectroscopy and Spectrometric Calibration

To evaluate the specific activity concentrations of ^{226}Ra, ^{232}Th, and ^{40}K in the granite samples, high-resolution gamma-ray spectroscopy was conducted using a laboratory-shielded High-Purity Germanium (HPGe) coaxial detector (Canberra, model GR4020). The detection system possesses a relative efficiency of 40% and a certified energy resolution (FWHM) of 1.95 keV at the 1332 keV photo peak of ^{60}Co. To eliminate ambient background radiation contributions, the detector was isolated within a 6.22-cm-thick cylindrical lead shield lined internally with an internal carbon composite lining. The resulting detector signals were processed via a spectral amplifier (Canberra, model 2002CSL), and spectrum acquisition was maintained for an optimized duration of 30,000 seconds per sample to ensure adequate counting statistics and account for background noise. Ambient background radiation was concurrently quantified and corrected by measuring identical empty cylindrical containers under identical operational setups. Spectral data analysis and peak evaluation were executed via Genie 2000 software (Canberra, USA). Potential spectral interferences were meticulously resolved; specifically, the specific activity of ^{226}Ra was determined from its 186.2 keV photo peak by mathematically subtracting the overlapping 185.7 keV gamma line of ^{235}U using standard nuclear cross-talk equations.

To ensure the utmost reliability of the generated spectrometric data, the detection system underwent a comprehensive two-phase standardization protocol encompassing both energy alignment and efficiency characterization. The former was implemented to derive a definitive linear relationship between the pulse-height channels and their corresponding photon energies across a broad spectral window spanning from 100 keV to 2600 keV, thereby facilitating the accurate identification of all relevant photo peaks. Subsequently, efficiency calibration was executed to quantify the detector's response function using both mathematical modeling and empirical validation. Mathematical efficiency calibration was performed utilizing LabSOCS software, which models crucial parameters including sample-detector geometry, sample density, elemental composition, and container properties based on factory measurements. The software validation was achieved using certified reference standards (IAEA, RG-set) that exhibit physical characteristics, particularly bulk density, congruent with the granite matrices under study. To eliminate potential geometric biases and minimize self-absorption errors, a rigorous source-to-detector configuration was maintained, ensuring that the reference materials and the experimental samples were analyzed under identical spatial orientations. The empirical validation yielded a high correlation between mathematical and empirical efficiencies, with a variance consistently below 10%.

Theoretical Calculations:

Concentration of Radionuclides: The radionuclide concentrations of ^{226}Ra, ^{232}Th and ^{40}K were calculated in units of (Bq.kg^{-1}) (Al-abrdi et al., 2025), (Salha et al., 2023):

$$A_n = \frac{C_n - C_b}{\varepsilon\, I_\gamma\, t\, m} \qquad (1)$$

The specific activity (A_n) of each radionuclide is determined based on the net count rate derived from the sample counts (C_n) and background counts (C_b) in CPS, taking into account the detection efficiency (ε), the gamma-ray emission probability (I_γ), the measurement duration (t), and the sample mass (m).

Representative Level Index (RLI)

The Representative Level Index (RLI) is employed to evaluate the gamma radiation levels associated with specific radionuclides. It is mathematically defined as follows:

$$RLI= A_{Ra}/150 + A_{Th}/100+ A_K/1500 \quad (2)$$

Where A_{Ra}, A_{Th}, and A_K denote the activity concentrations of Ra-226, Th-232 and K-40 in (Bq/Kg), respectively. This radiation hazard index serves to assess the radiological risk posed by natural terrestrial radionuclides within the analyzed samples. For the environment to be considered radiologically safe for human health, the RLI value must remain below the unity threshold (RLI < 1) (Hamza et al., 2019).

Activity Utilization Index (AUI)

To evaluate the air dose rates effectively, the Activity Utilization Index (AUI) is calculated for various groups of the three primary radionuclides. This index is expressed by the following equation:

$$AUI = f_{Ra}\left(\frac{A_{Ra}}{50}\right) + f_{Th}\left(\frac{A_{Th}}{50}\right) + f_K\left(\frac{A_K}{500}\right) \quad (3)$$

In this expression, f_{Ra}, f_{Th} and f_K represent the fractional dose contributions to the total airborne dose rate arising from the gamma radiation of ^{226}Ra, ^{232}Th, and ^{40}K, respectively. The AUI provides a standardized measure to assess the actual radiological impact based on the specific activity concentrations found within the samples. The standard values of f_{Ra}, f_{Th} and f_K are 0.462, 0.604, and 0.0417, respectively (Kolo et al., 2015).

Concentration Index (I_c)

The gamma activity concentration index (I_c), expressed in Bq \kg^{-1}, is estimated utilizing the following empirical relation (Dallner M., 2000), (Salha et al., 2023):

$$I_c = \left(\frac{A_{Ra}}{300}\right) + \left(\frac{A_{Th}}{200}\right) + \left(\frac{A_K}{3000}\right) \quad (4)$$

Representative Alpha Index (I_α)

The potential alpha radiation hazard, arising from the inhalation of radon progeny exhaled from the investigated samples, is assessed via the Alpha Index (I_α). To ensure radiological safety, this index should ideally be less than unity. It is calculated as follows (Salha et al., 2023):

$$I_\alpha = \left(\frac{A_{Ra}}{200}\right) \quad (5)$$

Annual Gonadal Equivalent Dose (AGDE)

The United Nations Scientific Committee on the Effects of Atomic Radiation (UNSCEAR) emphasizes the high radiosensitivity of specific organs, including the gonads, bone marrow, and bone surface cells. An increase in the Annual Gonadal Equivalent Dose (AGDE) is known to adversely affect bone structures and hematopoietic functions within the bone marrow. The AGDE value is derived from the activity concentrations of ^{226}Ra, ^{232}Th, and ^{40}K using their respective weighting factors to evaluate the overall radiological impact on these sensitive tissues (Hassan et al., 2010), (Asma et al., 2023).

$$\text{AGDE } (\mu Svy^{-1}) = 3.095 A_{Ra} + 4.18\, A_{Th} + 0.314\, A_K \quad (6)$$

The conversion factors (3.095, 4.18, and 0.314) represent the dose rate delivered to the gonads per unit of activity concentration for each radionuclide.

RESULTS

Radium-226's specific radioactivity was evaluated by measuring its gamma rays at 186.1 keV (after deducting 185.7 keV from uranium-235). The particular radioactivity of thorium-232 was assessed using the energies of 338.4, 911.2, and 968.9 keV from actinium-228, along with 583 keV from thallium-208. Potassium-40 was assessed with 1460.8 keV of potassium.

The experimental data presented in Table 2 demonstrate that the specific activity concentrations of ^{226}Ra in the investigated granite samples are exceptionally high, ranging from 2089.59 Bq•kg^{-1} (sample G4) to 2737.37 Bq•kg^{-1} (sample G3), with a grand mean of 2398.23 Bq•kg^{-1}. These values exceed the world standard average background limit (32 Bq•kg^{-1}) by approximately 65 to 85 times. Similarly, ^{232}Th and ^{40}K mean values (82.23 Bq•kg^{-1} and 1244.33 Bq•kg^{-1}, respectively) are markedly above international reference baselines, as shown in Figure 2. This prominent radiological anomaly is strictly governed by local geological and mineralogical features (Saleh et al., 2025). The collection quarries are situated in well-documented younger granite shear zones in the Eastern Desert of Egypt, where high-temperature late-magmatic hydrothermal alterations have led to the exceptional concentration of highly radioactive refractory accessory minerals such as zircon, monazite, allanite, uranothorite, and apatite which are trapped within the crystalline silicate framework of the granite rocks (Shereif et al., 2026).

Table (2). Activity concentrations (Bq.kg^{-1}) of ^{226}Ra, ^{232}Th and ^{40}K.

Sample	Ra-226	Th-232	K-40
G1	2564.87	82.79	1309
G2	2258.98	81.66	1195
G3	2737.37	79.52	1254
G4	2089.59	71.85	1162
G5	2316.73	89.12	1264
G6	2421.83	88.43	1282
Average	2398.228	82.22833	1244.333
P.L.	32	45	420

P.L.: The internationally permissible limits according to the reference United Nations Scientific Committee on the Effects of Atomic Radiation 2010 (UNSCEAR 2010).

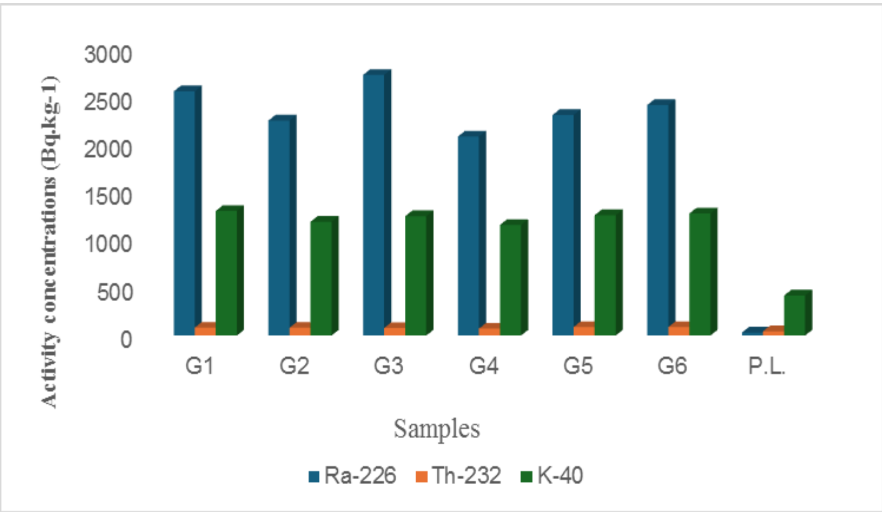

Figure (2). Activity concentrations of the samples.

Radiological Hazard Assessment and Health Risk Indices

To comprehensively evaluate the potential radiological risks associated with the granite samples from the study area, several hazard indices were calculated and are summarized in Table 3. The assessment included the Representative Level Index (RLI), Activity Utilization Index (AUI), Concentration Index (Ic), and Alpha Index (Iα), alongside the Annual Gonadal Dose Equivalent (AGDE).
As presented in Table 3, all calculated parameters for the six investigated samples significantly exceed the international safety benchmarks established by UNSCEAR (2010). The evaluated health risk indices compiled in Table 3 strongly match the high activity levels. The Gamma Representative Level Index (RLI) averages 17.64, which is significantly above the unity safety limit (RLI < 1.0), indicating that the materials could cause a significant excess in standard ambient indoor dose rates. Crucially, the Annual Gonadal Dose Equivalent (AGDE) values range from 7132.48 to 9198.31 $\mu Sv \cdot y^{-1}$, with an overall mean of 8156.95 $\mu Sv \cdot y^{-1}$. Comparing this with the globally accepted baseline of 300 $\mu Sv \cdot y^{-1}$ reveals an increase of approximately 27-fold. This suggests that long-term, unmitigated exposure to these premium granites in confined environments could lead to significant cumulative gonadal and bone-marrow exposures (Moghazy et al., 2021). Consequently, while these granite varieties possess exceptional mechanical and structural longevity, their installation in large surface areas within residential dwellings must be restricted, and they should instead be used in open-air public plazas or external commercial cladding where proper ventilation minimizes potential radiological risks.

The significantly elevated specific activity concentrations of ^{226}Ra observed in the studied granite varieties from the Eastern Desert can be geologically justified by the intense hydrothermal alteration processes characteristic of this region. According to Abd El-Halim et al. (2017), granitic plutons in the Eastern Desert of Egypt frequently act as host rocks for primary uranium and thorium mineralizations. In these tectonic zones, the granite undergoes strong structural and mineralogical alterations, notably quartz dissolution (episyenitization). This process yields a highly porous rock matrix filled with micro-cavities and fractures, creating ideal traps for the concentration and precipitation of secondary uranium mineralization and its decay products, including ^{226}Ra (Abd El-Halim et al., 2017). Furthermore, since the samples are stored to achieve secular radioactive equilibrium, the high concentration of radium directly mirrors the abundance of parent uranium isotopes trapped within these altered granitic structures, which explains why the radiological hazard indices, such as the Annual Gonadal Dose Equivalent (AGDE), drastically exceed the global safety limits (Figure 3).

Table (3). Calculated Environmental External Radiological Hazard Indices.

Sample	RLI	AUI	I_C	I_α	AGDE ($\mu Sv.y^{-1}$)
G1	18.7997	24.80867	9.39985	12.82435	8695.361
G2	16.67313	21.95909	8.336567	11.2949	7708.112
G3	19.88033	26.35848	9.940167	13.68685	9198.31
G4	15.42377	20.27267	7.711883	10.44795	7132.482
G5	17.17873	22.58857	8.589367	11.58365	7939.697
G6	17.8845	23.55286	8.94225	12.10915	8267.74925
Average	17.64003	23.25673	8.820014	11.99114	8156.951792
P.L.	<1	<1	<1	<1	300

P.L.: The internationally permissible limits according to the reference (UNSCEAR 2010).

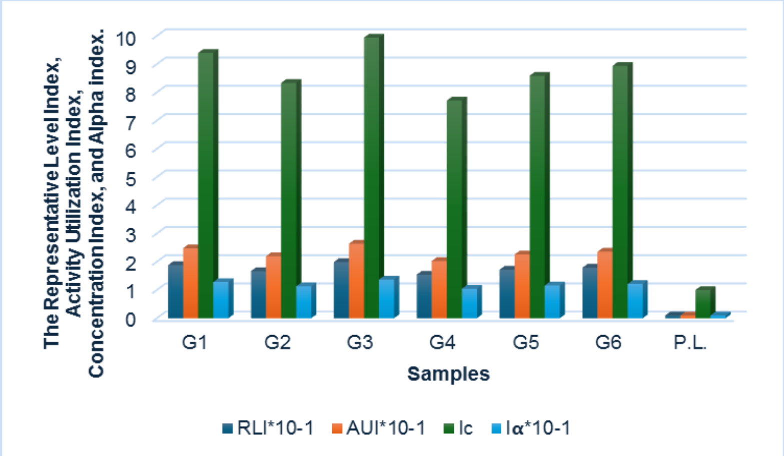

Figure (3). The Representative Level Index (Bq.kg^{-1}), Activity Utilization Index (Bq/kg), Concentration Index (Bq/kg), and Alpha Index (Bq/kg).

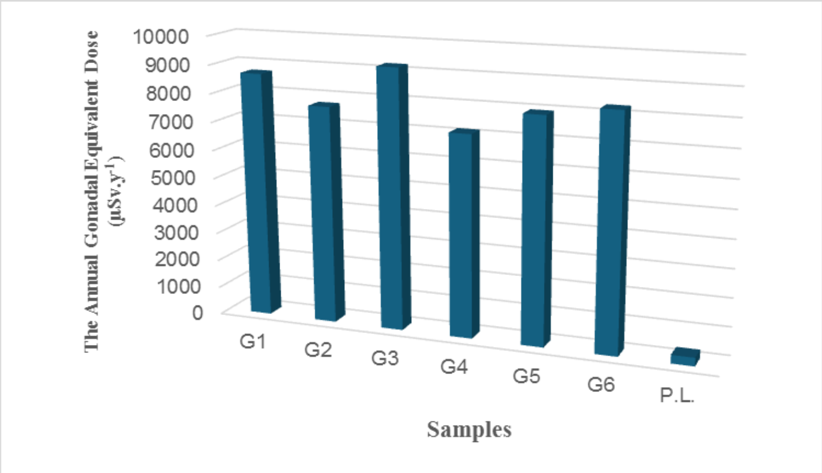

Figure (4). The Annual Gonadal Equivalent Dose (μSv.y^{-1}).

As can be seen from Table 3 and Figure 4, the annual equivalent dose to the reproductive gonads exceeded the internationally accepted limit in all samples.

The highest value was found in sample 3, while sample 4 had the lowest value among the measured samples.

CONCLUSION

his study provides a rigorous and comprehensive evaluation of natural radioactivity concentrations and the associated external radiological risks of commercial Egyptian granite varieties. Utilizing a high-resolution High-Purity Germanium (HPGe) gamma-ray spectrometry system, configured with precise ambient background subtraction and calibrated via certified international reference standards, the specific activity concentrations of ^{226}Ra, ^{232}Th, and ^{40}K were determined with high analytical precision. The experimental results demonstrate that the radioactivity concentrations across all investigated samples markedly exceed internationally recognized permissible baseline safety limits.

This pronounced radiological elevation is directly governed by late-magmatic hydrothermal processes and unique accessory mineral configurations localized within the Eastern Desert quarries. According to Abd El-Halim et al. (2017), granitic plutons within the Eastern Desert of Egypt (such as the Gabal Gattar intrusion) frequently host primary uranium and thorium mineralizations. In these active tectonic shear zones, the granitic rocks have undergone intensive structural and mineralogical alterations, characterized predominantly by quartz dissolution, a process known as episyenitization. This phenomenon yields a highly porous silicate matrix abundant in micro-cavities and fractures, creating optimal geochemical traps for the secondary concentration and subsequent precipitation of uranium minerals and their respective decay progeny, including ^{226}Ra (Abd El-Halim et al., 2017). Given that the experimental samples were stored to achieve complete secular radioactive equilibrium prior to measurement, the exceptionally high specific activities of ^{226}Ra directly reflect the substantial abundance of parent radionuclides trapped within these hydrothermally altered crystalline structures.

Consequently, the calculated environmental hazard indices, most notably the Annual Gonadal Dose Equivalent (AGDE), which yielded a striking average of 8156.95 µSvy$^{-1,}$ drastically exceed global safety baselines. Because these rigid plutonic stones serve exclusively as structural and decorative building elements rather than entering biological ingestion pathways, the principal threat is strictly limited to cumulative external gamma exposure. In conclusion, the investigated granite varieties demand stringent radiological monitoring and regulatory oversight. To mitigate potential public health risks and ensure human safety, it is highly recommended to restrict their application in confined, poorly ventilated residential spaces, favoring instead their utilization in outdoor architectural cladding, structural facades, or well-ventilated public infrastructure projects.

Duality of interest: The authors declare that they have no duality of interest associated with this manuscript.

Author contributions: Asma M.A. Othman developed the theoretical formalism and supervised the project. Areej I. Hazawi and Salha D. Alsaadi performed the analytic calculations and numerical simulations. All authors contributed to the review, editing, and final approval of the manuscript.

Funding: the authors did not receive funding (institutional, private and/or corporate financial support) for the work reported in their manuscript.

REFERENCES

Abd El-Halim, E., El-Dine, N. W., El-Bahi, S. M., El-Aassy, I. E., El-Sheikh, E. M., Al-Abrdi, A. M. J. N. P., & Energy, A. (2017). Excessive Lifetime Cancer Risk and Natural Radioactivity Measurements of Granite and Sedimentary Rock Samples. *18*(4), 371. https://doi.org/https://doi.org/10.15407/jnpae2017.04.371

AL-abrdi, A. M. A., Hazawi, A., Abd-Alhamid, M. A., & Yousif, R. J. S. U. S. J. (2025). Evaluation of the activity levels and the radiological hazards associated with the imported chemical fertilizers used in Libya. *15*(2), 26-32.

Al-Abrdi, A. M. J. L. J. o. B. S. (2023). Measurements of natural radioactivity and evaluation of radiation hazard indices in Barley Samples in Libya Markets. *20*(2), 51-64.

Alsaadi, S., Hazawi, A., & Elmzainy, A. S. J. S. J. f. F. o. S.-S. U. (2023). Assessment of radioactivity in the soil samples from Al Bayda city, Libya, and its radiological implications. *3*(1), 18-23. https://doi.org/https://doi.org/10.37375/sjfssu.v3i1.1058

Dallner, M., Elo, A.-L., Gamberale, F., Hottinen, V., Knardahl, S., Lindström, K.,…Ørhede, E. (2000). Validation of the General Nordic Questionnaire (QPSNordic) for psychological and social factors at work.

Hamza, Z. M., Kadhim, S. A., & Hussein, H. H. (2019). Assessment the norms for agricultural soils in Ghammas town, Iraq.

Hassan, N., Ishikawa, T., Hosoda, M., Sorimachi, A., Tokonami, S., Fukushi, M.,…chemistry, n. (2010). Assessment of the natural radioactivity using two techniques for the measurement of radionuclide concentration in building materials used in Japan. *283*(1), 15-21. https://doi.org/https://doi.org/10.1007/s10967-009-0050-6

Kolo, M. T., Aziz, S. A. B. A., Khandaker, M. U., Asaduzzaman, K., Amin, Y. M. J. E. S., & Research, P. (2015). Evaluation of radiological risks due to natural radioactivity around Lynas Advanced Material Plant environment, Kuantan, Pahang, Malaysia. *22*(17), 13127-13136. https://doi.org/https://doi.org/10.1007/s11356-015-4577-5

Moghazy, N. M., El-Tohamy, A. M., Fawzy, M. M., Awad, H. A., Zakaly, H. M., Issa, S. A., & Ene, A. J. A. S. (2021). Natural radioactivity, radiological hazard and petrographical studies on aswan granites used as building materials in Egypt. *11*(14), 6471. https://doi.org/https://doi.org/10.3390/app11146471

Saleh, G. M., Semary, H. E., Lasheen, E. S. R., Kamar, M. S., Elkelish, A., Sami, M.,…Abdelaal, A. J. F. i. E. S. (2025). Metal contamination and radiological risk assessment in the coastal zone of Wadi Ghadir outlet, Red Sea, Egypt. *13*, 1667069. https://doi.org/https://doi.org/10.3389/fenvs.2025.1667069

Shereif, A. S., Heikal, M. T. S., El Ela, A. S. A., El Shabasy, A., Masoud, A. E., & Csámer, Á. J. S. R. (2026). Gamma activity concentrations of 226Ra, 232Th, 40K, and health hazard assessments of granites from Wadi El-Nabi'mining area, Egyptian Nubian Shield. *16*(1), 9122. https://doi.org/https://doi.org/10.1038/s41598-026-39664-4

UNSCEAR, United Nations Scientific Committee on the Effect of Atomic Radiation, (2010): "Sources and Effects of Ionizing Radiation". Report to General Assembly with Scientific Annexes, United Nations, New York.